

Electron Spin Resonance

Anusha Fatima Alam (1009056539) and Hyunji Kim (1008822552)

April 11th, 2024

Abstract

The objective of this practical is to experimentally determine the Landé factor, g , using the electron spin resonance measurements. The set-up comprises of a pair of Helmholtz coils that generate a uniform homogeneous magnetic field, and Leybold boxes that contain the ESR Basic Unit and the ESR Adapter which control the RF fields and connections. The experimental procedure involves manually tuning the frequency and current to observe resonance and collecting the relevant data points across different frequency ranges. The gyromagnetic ratios for the small, medium, and large coils were determined to be $(158.7 \pm 4.7) \times 10^9$, $(149.4 \pm 3.0) \times 10^9$, and $(147.8 \pm 2.8) \times 10^9$, respectively. Additionally, the calculated Landé g -factors for the small, medium, and large coils were 1.80 ± 0.05 , 1.70 ± 0.03 , and 1.68 ± 0.03 , respectively. Potential errors in this lab include inconsistencies in positioning the DPPH sample within the coils, fluctuations in the uniformity of the magnetic field generated by the Helmholtz coils, and variations in the RF field strength due to imprecise control settings on the ESR Basic Unit.

1 Introduction

Electron spin is a term used to describe the intrinsic angular momentum of the electron. When molecules of solid exhibit paramagnetism (due to presence of unpaired electron spins), transitions can be induced between the distinct spin states by first applying a magnetic field followed by supplying electromagnetic energy (typically in the microwave range of frequencies). The resulting absorption spectra is described as the electron spin resonance which will be used to experimentally determine the Landé factor, g . Every electron spin is combined with a magnetic moment. This is intuitive when an electron is treated as a rotating electrical charge and recall that an electrical circuit has a magnetic moment. Since an electron has a negative charge, its magnetic moment opposes the spin.

Electrons "spinning" on their axis have a magnetic dipole moment $\vec{\mu}$. When there is a magnetic field present, it will have a potential energy:

$$E = -\vec{\mu} \cdot \vec{B} \quad (1)$$

The magnetic moment $\vec{\mu}$ is proportional to the spin angular momentum \vec{S} and gyromagnetic ratio γ .

$$\vec{\mu} = \gamma \vec{S} \quad (2)$$

If we only consider the z-component of the magnetic field, the potential energy of an electron is:

$$E = \mu_z B_z = \gamma S_z B_z = \pm \frac{1}{2} \gamma \hbar B_z \quad (3)$$

From quantum mechanics, $S_z = \pm \frac{\hbar}{2}$. The difference in the two energies is:

$$\Delta E = \gamma \hbar B_z \quad (4)$$

When a photon with this energy difference incident on an electron in the lower energy state, the photon may be absorbed and the orientation of the electron may flip. This phenomenon is so called **electron spin resonance**. Equation 4 can be rewritten using photon energy $h\nu$:

$$\nu = \frac{1}{2\pi} \gamma B_z \quad (5)$$

If an electron has a homogeneous charge distribution, γ is expected to be $\frac{e}{2m}$, where e and m are the charge and mass of the electron, respectively. But since real electrons have a larger $\vec{\mu}$ than the expectation, the difference between the values can be represented using the Landé g factor:

$$g = \frac{\gamma}{e/2m} > 1 \quad (6)$$

The goal of this experiment is to determine Landé g -factor. In chemical free radicals, that a molecule has at least one unpaired valance electron, these substances are paramagnetic. The free radical used in this experiment is diphenylpicryl hydroxyl (DPPH). Since theses unpaired electrons are not influenced by their orbital motion, they can be used to obtain a good value for the free electron gyromagnetic ratio and Lande g -factor.

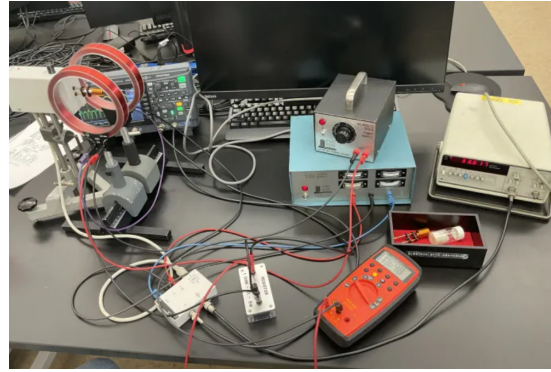
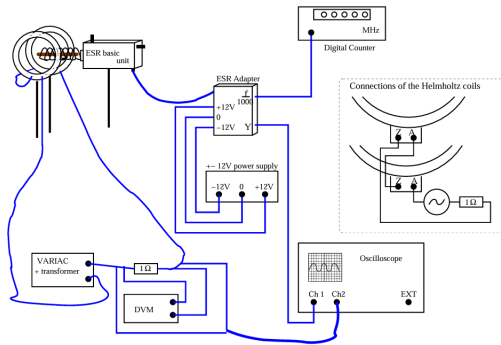
A magnetic field is generated using the Helmholtz coils. As the field hits the resonance point the absorption of the high-frequency photons may be observed. The equation for the central field generated by a pair of coils is given by:

$$B = \left(\frac{4}{5}\right)^{\frac{3}{2}} \frac{\mu_0 n I}{R} \quad (7)$$

Where $\mu_0 = 4\pi \times 10^{-7} \text{ (N/A}^2\text{)}$, R is the radius of the coils, n is the number of turns, and I is the current through the coils. Note that since the Helmholtz coils are connected parallel, the current through the coils is half of the current measured. According to the data sheet, $R = 6.7 \text{ cm}$ and $n = 320$ [3].

2 Materials and Methods

2.1 Materials



(a) Schematic Diagram of the instrument wiring for the (b) Photo of the set-up with wires manually connected to Electron Spin Resonance Lab using AC-method measure-the apparatus as shown in the schematic on the left. The ment. The blue lines indicate the connecting cables. AC current and frequency measurements were recorded.

Figure 1: Experimental Set-up. The apparatus comprised two Leybold boxes: the ESR Basic Unit, housing a copper coil and controls for RF field strength and frequency, and the ESR Adapter, facilitating connections to power supplies and oscilloscope. Helmholtz coils generated a uniform magnetic field for ESR measurements.

Apparatus (refer to figure 1 for the experimental set-up):

- Helmholtz Coils
- Oscilloscope
- Frequency Counter ($\pm 0.005 \text{ MHz}$)
- Triple Output Power Supply
- Ammeter ($\pm 0.005 \text{ A}$)
- 1 Ohm Resistor
- Adjustable clamp with holder
- ESR Probe Unit
- DPPH Sample
- Plug-in Coils (Small, Medium and Large)

2.2 Method

The small, medium and large plug-in coil were plugged in respectively in the ESR basic unit and the DPPH sample was inserted inside the plug-in coil. The helmholtz coil were connected in parallel to the ESR unit and mounted such that the DPPH sample was in the middle of the coil and was perpendicular to their common axis and such that the external magnetic field B_z is perpendicular to the copper coil's axis. This ensured that along the axis the magnetic field maintains homogeneous. The power supplies, ammeter, oscilloscope, frequency counter, and other remaining circuit components were connected as depicted in Figure 1a.

The power supplies, ammeter, and the ESR basic unit were activated. The ammeter is initialized into AC mode, and the current was regularly monitored to ensure that it does not exceed 2 amperes through the coils. The oscilloscope was configured for initial triggering. The current going into the coils was monitored both using the ammeter and the voltage drop across the supplied $1\ \Omega$ resistor with the oscilloscope.

The frequency and current were adjusted until the two peaks on the oscilloscope merged into one, indicating resonance. The RF frequency and AC current were measured with respective uncertainties quantified using the uncertainty propagation described in section 4. The current and frequency were continuously varied to identify new resonance frequencies and collect additional data points. Exactly 5 data points were recorded for each of the three plug-in coils, which covered a wide frequency range.

3 Data and Analysis

Rearranging 5, the equation used to determine the gyromagnetic ratio is:

$$\gamma = \frac{2\pi\nu}{B_z} \quad (8)$$

Based on the observed frequency and current values, the magnetic fields are determined using Equation 7. Subsequently, the average gyromagnetic ratio and Landé g-factor are calculated according to Equations 6 and 8, respectively, and summarized in Table 1, including uncertainties expressed as one standard deviation. According to Equation 5, the angular frequency is directly proportional to B_z , with the proportionality constant $\frac{\gamma}{2\pi}$. The correlation between the angular frequency ν and the magnetic field B_z is graphically represented by multiplying 2π to both sides of the equation 5, including the slope, intercept, and residuals of the plot. Furthermore, both R-squared and chi-squared values are computed and reported to assess the goodness of fit.

Table 1: Calculated gyromagnetic ratio and Landé g-factor

Coil	Gyromagnetic ratio $[\gamma \times 10^9]$	Landé g-factor
Small	158.7 ± 4.7	1.80 ± 0.05
Medium	149.4 ± 3.0	1.70 ± 0.03
Large	147.8 ± 2.8	1.68 ± 0.03

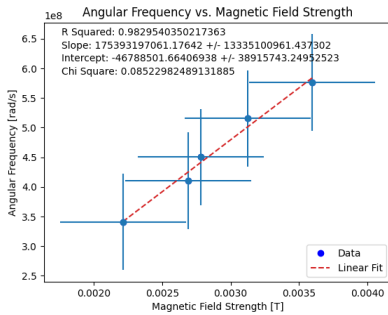


Figure 2: Angular Frequency vs. Magnetic Field Strength of the Small Coil

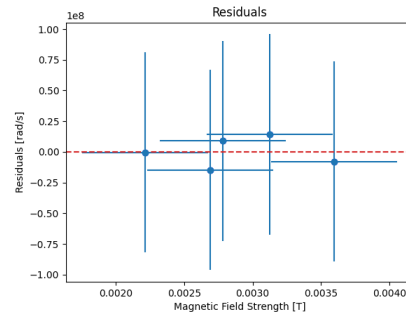


Figure 3: Residuals Plot of the Small Coil

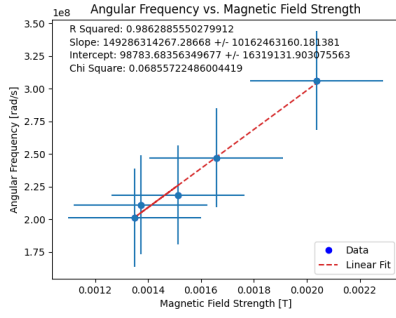


Figure 4: Angular Frequency vs. Magnetic Field Strength of the Medium Coil

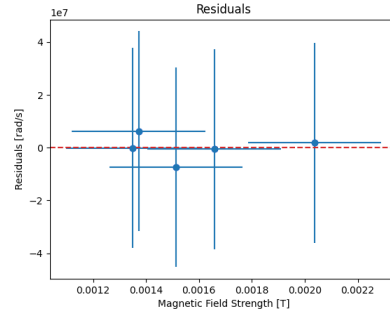


Figure 5: Residuals Plot of the Medium Coil

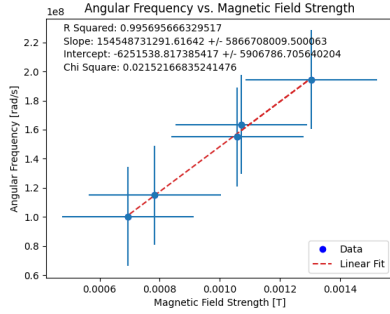


Figure 6: Angular Frequency vs. Magnetic Field Strength of the Large Coil

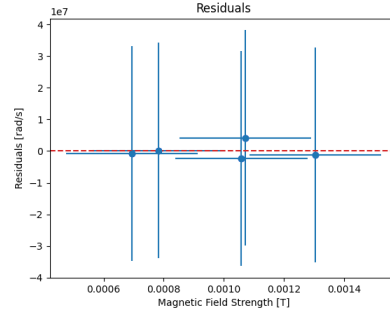


Figure 7: Residuals Plot of the Large Coil

The theoretical value of the gyromagnetic ratio is $\gamma = 1.759 \times 10^{11} [\frac{C}{kg}]$, and the experimental slope should align with this value. Given that Equation 5 predicts no intercept, the theoretical intercept should be zero. Upon comparing the experimental slopes and intercepts with the theoretical values, the slopes for the small, medium, and large configurations were found to be $(175.4 \pm 13.3) \times 10^9 [\frac{rad}{s \cdot T}]$, $(149.3 \pm 10.2) \times 10^9 [\frac{rad}{s \cdot T}]$, and $(154.5 \pm 5.9) \times 10^9 [\frac{rad}{s \cdot T}]$, respectively. These values demonstrate consistency with the theoretical gyromagnetic ratio of 1.759×10^{11} .

Additionally, the intercepts were determined to be $(-46.8 \pm 38.9) \times 10^6 [\frac{rad}{s \cdot T}]$, $(0.098 \pm 16.3) \times 10^6 [\frac{rad}{s \cdot T}]$, and $(-6.25 \pm 5.91) \times 10^6 [\frac{rad}{s \cdot T}]$ for the small, medium, and large configurations, respectively. These results indicate that the intercepts do not consistently align with the theoretical value of zero.

The coefficients of determination (R^2) for the small, medium, and large coils were 0.983, 0.986, and 0.996, respectively, suggesting that the linear regression models approximate the empirical data with high precision. Furthermore, the chi-squared values for the small, medium, and large coils were 0.085, 0.069, and 0.022, respectively. The chi-squared values for the small and medium coils fall below $\alpha = 0.1$, indicating that the model is valid at an 80% confidence level, whereas the value for the large coil, being below $\alpha = 0.05$, confirms validity at a 90% confidence level.

Therefore, the linear regression model effectively predicts the empirical data, though improvements could be made to achieve better alignment with the theoretical intercepts.

4 Uncertainty Propagation

4.1 Uncertainty in Gyromagnetic Ratio

Combining equation 7 and 8, the equation for the gyromagnetic ratio can be written as:

$$\gamma = \frac{2\pi\nu R}{\mu_0 n I} \left(\frac{5}{4}\right)^{\frac{3}{2}} \quad (9)$$

Therefore, the uncertainty in gyromagnetic ratio is given by [2]:

$$\frac{\delta\gamma}{\gamma} = \sqrt{\left(\frac{\delta\nu}{\nu}\right)^2 + \left(\frac{\delta I}{I}\right)^2} \quad (10)$$

Where $\delta\nu$ is the experimental uncertainty for the frequency and δI is the experimental uncertainty for the current.

4.2 Uncertainty in Landé g-factor

Since the equation for the Landé g-factor 6, the uncertainty in the Landé g-factor is given by [2]:

$$\frac{\delta g}{g} = \sqrt{\left(\frac{\delta\gamma}{\gamma}\right)^2} \quad (11)$$

Where $\delta\gamma$ is the estimated error in the gyromagnetic ratio calculated using 10.

4.3 Uncertainty in Linear Fit

Let y the linear function of x given by $y = mx + b$, unknown parameters m and b is given by [5]:

$$\begin{aligned} \Delta &= N \sum x_i^2 - \left(\sum x_i\right)^2 \\ m &= \frac{N \sum_{i=1}^N x_i y_i - \sum_{i=1}^N x_i \sum_{i=1}^N y_i}{\Delta} \\ b &= \frac{\sum_{i=1}^N y_i - m \sum_{i=1}^N x_i}{N} \end{aligned} \quad (12)$$

Where N measurements result in N pairs of numbers x_i and y_i .

The uncertainties in m and b are given by the standard deviations s_m and s_b , respectively, [5]:

$$\begin{aligned} s_{y,x}^2 &= \frac{1}{N-2} \sum [y_i - (b + mx_i)]^2 \\ s_m &= \sqrt{N \frac{s_{y,x}^2}{\Delta}} \\ s_b &= \sqrt{\frac{s_{y,x}^2 \sum x_i^2}{\Delta}} \end{aligned}$$

The coefficient of determination R^2 is given by [5]:

$$R^2 = 1 - \frac{(N-2)s_{y,x}^2}{\sum (y_i - \bar{y})^2} = 1 - \frac{(N-2)s_{y,x}^2}{\sum (y_i - \frac{y_i}{N})^2} \quad (13)$$

The chi-squared value is given by [4]:

$$\chi^2 = \sum \frac{(O_i - E_i)^2}{E_i} \quad (14)$$

Where O_i is the observed value and E_i is the expected value.

5 Discussion

5.1 Uncertainty Determination of the Merged Dips

There is certainly uncertainty in determining when the two dips merge. This uncertainty arises due to several reasons. Firstly, the exact definition of when two peaks merge can vary depending on the measurement criteria chosen, such as the point at which the peaks reach half-maximum height or when they visually appear to merge. Because visual inspection vary from person to person is very subjective, there is certainly a large potential for experimental uncertainty. Secondly, there could be noise in the measurement and the instrumentation system, affecting the accuracy of identification of the merging point. Additionally, the assumption of resonance being precisely achieved at the point of merged dips might not hold true when subject to certain conditions, such as when there are non-linear effects or broadening of the resonance peak.

5.2 Asymmetric Behaviour of the ESR Signal

The ESR signal was be perfectly symmetric about the maximum current point and this behavior was observed due to various reasons. One fundamental cause is the presence of relaxation mechanisms within the sample material, leading to different rates of energy absorption and emission during the ESR process. Additionally, imperfections in the experimental setup or sample itself can introduce asymmetry in the signal. For instance, non-uniformity in the magnetic field or variations in the sample composition can affect the shape of the ESR signal.

In actuality, though, phase shift calibration errors could lead to asymmetry. The measurement signal undergoes a time delay that is detected as a phase shift on the oscilloscope as it moves from the ESR basic unit to the adaptor along the circuit. This will result in signal asymmetry if it is not corrected by the oscilloscope or the ESR adaptor. There are other potential causes of signal asymmetry, such as limitations in the experimental design and protocols. Asymmetrical signals, for instance, may result from the electrons in the sample experiencing distinct resonance conditions due to a spatial gradient in the magnetic field. Furthermore, the numerous DPPH molecules in the sample's tiny intermolecular interactions may cause the electrons to behave in an unpredictable way, further altering symmetry.

5.3 Relationship across wide range of Frequencies

The relationship described by Equation (7) may not hold true over a wide range of frequencies. While the equation provides a theoretical framework for calculating the magnetic field produced by the Helmholtz coils, deviations from linearity can occur in practical scenarios. Factors such as non-idealities in coil construction, magnetic material properties, and experimental conditions may introduce nonlinear effects. Therefore, it is essential to validate the linearity assumption through experimental verification across different frequency ranges.

From the analysis of the linear regression lines generated for the plots and residuals in figure 2 to 7 and using reduced chi-squared, we can conclude that the relation from Equation 4 appears to reflect the experimental results throughout a broad range of frequencies. This result, however, is not well supported because, as should be mentioned, extracting any significant relationships between frequency ν and magnetic field strength B may not be possible with only 5 data points. To validate this result, more data points across a larger range of frequencies should be gathered in subsequent experiment explorations.

5.4 Physical Interpretation of the Width of the Peak

The width of the resonance peak in ESR spectra corresponds to the range of frequencies over which the sample absorbs energy most efficiently. This width is influenced by several factors, including the homogeneity of the magnetic field, the relaxation times of the sample, and any broadening mechanisms present. A broader peak indicates a wider distribution of resonant frequencies within the sample, which could arise from variations in local magnetic environments or relaxation processes. Understanding the peak width provides insights into the dynamics and interactions occurring within the sample material.

By visually inspecting the resonance waveform, the width of the peak B can be physically described as the width of the absorption line from the resulting photon. In a homogeneous magnetic field, the line

width can be interpreted by the Heisenberg uncertainty principle as an expression of uncertainty of the energy, E , of the electron transition:

$$\Delta E \Delta T \geq \frac{\hbar}{2} \quad (15)$$

where ΔT refers to the lifetime of the level. Rearranging the equation above for $\hbar \nu$ and substituting it for E , the following expression can be determined:

$$\Delta B = \frac{h}{2g\mu_B \Delta T} \quad (16)$$

From this relationship, it can clearly be concluded that the line width B does not depend on the frequency, ν .

5.5 Operating the Basic Unit

The Basic Unit generates a high-frequency RF field inside the copper coil containing the sample material. The knob for controlling frequency is connected to adjust the frequency of the RF field. This parameter is then outputted from the Y socket, allowing monitoring of the absorption of high-frequency photons. Essentially, the Basic Unit facilitates the generation and control of the RF field necessary for performing Electron Spin Resonance (ESR) measurements, enabling the study of magnetic properties of the sample material.

6 Conclusion

In this experiment, the gyromagnetic ratio and the Landé g -factor values were calculated using Equations 8 and 6, respectively. The gyromagnetic ratios for the small, medium, and large coils were determined to be $(158.7 \pm 4.7) \times 10^9$, $(149.4 \pm 3.0) \times 10^9$, and $(147.8 \pm 2.8) \times 10^9$, respectively. Additionally, the calculated Landé g -factors for the small, medium, and large coils were 1.80 ± 0.05 , 1.70 ± 0.03 , and 1.68 ± 0.03 , respectively. Compared to the theoretical value $\gamma = 175.9 \times 10^9$, the calculated values deviate due to the reasons discussed in section 5.1.

References

- [1] PHY294, *Electron Spin Resonance*, 2024.
- [2] PHY294, *Error Analysis for 2nd Year Experimental Physics*, 2024.
- [3] *Instruction sheet 555 604 - LD didactic*.
- [4] Admin, *Chi-square test: How to calculate Chi-square using formula with example*, BYJUS, <https://byjus.com/maths/chi-square-test/>.
- [5] PHY294, *Uncertainties in linear fit*, 2024.

7 Appendix A: Raw Data

Table 2: Measured Current and Frequency Data of the Small Coil

	AC Current [A]	Frequency [MHz]
1	1.031	54.28
2	1.253	65.303
3	1.296	71.667
4	1.455	82.035
5	1.675	91.685

Table 3: Measured Current and Frequency Data of the Medium Coil

	AC Current [A]	Frequency [MHz]
1	0.639	33.615
2	0.705	34.802
3	0.628	32.038
4	0.772	39.315
5	0.949	48.721

Table 4: Measured Current and Frequency Data of the Large Coil

	AC Current [A]	Frequency [MHz]
1	0.499	26.023
2	0.608	30.929
3	0.493	24.669
4	0.365	18.308
5	0.323	15.942

8 Appendix B: Python Code

```

1 import numpy as np
2 import matplotlib.pyplot as plt
3 from scipy import constants
4
5 N = 320 # number of turns of coils
6 R = 6.7e-2 # radius of coils (m)
7 Mu = 4e-7*np.pi
8
9 class Coil:
10     def __init__(self, frequency, current):
11         self.frequency = frequency*(10**6) # MHz to Hz
12         self.current = current/2
13         self.B = (4/5)**(3/2)*(Mu*N*self.current/R)
14         self.gyro = self.frequency*2*np.pi/self.B
15         self.lande = 2*constants.m_e*self.gyro/constants.e
16         self.energy = constants.h*self.frequency
17         self.energyp = 0.5*self.gyro*constants.hbar*self.B
18         self.energyn = -0.5*self.gyro*constants.hbar*self.B
19
20     def std(self):
21         return np.std(self.lande)
22
23     def plot(self):
24         plt.title("Angular Frequency vs. Magnetic Field Strength")
25         plt.xlabel("Magnetic Field Strength [T]")
26         plt.ylabel("Angular Frequency [rad/s]")
27         plt.legend (loc="lower right")
28         plt.show()
29
30     def plot_nu(self):
31         plt.plot(self.B, 2*np.pi*self.frequency, "ob", label="Data")
32         plt.errorbar(self.B, 2*np.pi*self.frequency, xerr=np.std(self.B),
33                     ↪ yerr=np.std(2*np.pi*self.frequency), fmt="o", color="tab:blue")
34         p, cov = np.polyfit(self.B, 2*np.pi*self.frequency, 1, cov=True)
35         np.polyval(p, self.B)

```



```

35     plt.plot(self.B, p[0]*self.B + p[1], "--", color="tab:red", label="Linear Fit")
36     print ("Slope + Intercept : ", p)
37     print("Cov:", np.sqrt(np.diag(cov)))
38     plt.annotate("Slope: " + str(p[0]) + " +/- " + str(np.sqrt(np.diag(cov))[0]) ,
    ↪ xy=(0.05, 0.9) , xycoords="axes fraction")
39     plt.annotate("Intercept: " + str(p[1]) + " +/- " + str(np.sqrt(np.diag(cov))[1]),
    ↪ xy=(0.05, 0.85), xycoords="axes fraction")
40
41     def chi_square(self):
42         p, cov = np.polyfit(self.B , 2*np.pi*self.frequency, 1, cov=True)
43         np.polyval(p, self.B)
44         chi_square = 0
45         for i in range(len(self.B)):
46             chi_square += (2*np.pi*self.frequency[i] - (p[0]*self.B[i] +
    ↪ p[1]))**2/(np.std(2*np.pi*self.frequency))**2
47         print("Chi Square: ", chi_square)
48         plt.annotate("Chi Square: " + str(chi_square), xy=(0.05, 0.8), xycoords="axes
    ↪ fraction")
49
50     def r_squared(self):
51         p, cov = np.polyfit(self.B , 2*np.pi*self.frequency, 1, cov=True)
52         np.polyval(p, self.B)
53         y_bar = np.average(2*np.pi*self.frequency)
54         sstot = 0
55         ssres =0
56         for i in range(len(self.B)):
57             sstot += (2*np.pi*self.frequency[i] - y_bar)**2
58             ssres += (2*np.pi*self.frequency[i] - (p[0]*self.B[i] + p[1]))**2
59             r_squared = 1 - ssres/sstot
60         print ("R Squared : ", r_squared )
61         plt.annotate("R Squared: " + str(r_squared), xy=(0.05, 0.95), xycoords="axes
    ↪ fraction")
62
63     def residuals(self):
64         p, cov = np.polyfit(self.B , 2*np.pi*self.frequency, 1, cov=True)
65         np.polyval(p, self.B)
66         plt.plot(self.B , 2*np.pi*self.frequency - (p[0]*self.B+p[1]), "ob")
67         plt.errorbar(self.B , 2*np.pi*self.frequency - (p[0]*self.B + p[1]),
    ↪ xerr=np.std(self.B), yerr=np.std(2*np.pi*self.frequency), fmt="o",
    ↪ color="tab:blue")
68         plt.title ("Residuals")
69         plt.xlabel("Magnetic Field Strength [T]")
70         plt.ylabel ("Residuals [rad/s]")
71         plt.axhline(y=0, color="tab:red", linestyle="--")
72         plt.show()
73
74     small = Coil(np.array([54.28,65.303,71.667,82.035,91.685]),
    ↪ np.array([1.031,1.253,1.296,1.455,1.675]))
75     med = Coil(np.array([33.615,34.802,32.038,39.315,48.721]),
    ↪ np.array([0.639,0.705,0.628,0.772,0.949]))
76     big = Coil(np.array([26.023,30.929,24.669,18.308,15.942]),
    ↪ np.array([0.499,0.608,0.493,0.365,0.323]))
77
78     # small
79     print("Spin Gyromagnetic Ratio (small): ", np.average(small.gyro), "+/-",
    ↪ np.std(small.gyro) )
80     small.plot_nu()
81     small.chi_square()
82     small.r_squared()
83     print("Lande g factor (small): ", np.average(small.lande), "+/-", np.std(small.lande))
84     small.plot()
85     small.residuals()

```

```

86 print(small.B)
87
88 # med
89 print("Spin Gyromagnetic Ratio (med): ", np.average(med.gyro), "+/-", np.std(med.gyro) )
90 med.plot_nu()
91 med.chi_square()
92 med.r_squared()
93 print("Lande g factor (med): ", np.average(med.lande), "+/-", np.std(med.lande))
94 med.plot()
95 med.residuals()
96 print(med.B)
97
98 # big
99 print("Spin Gyromagnetic Ratio (big): ", np.average(big.gyro), "+/-", np.std(big.gyro) )
100 big.plot_nu()
101 big.chi_square()
102 big.r_squared()
103 print("Lande g factor (big): ", np.average(big.lande), "+/-", np.std(big.lande))
104 big.plot()
105 big.residuals()
106 print(big.B)

```